Optics Communications 435 (2019) 145–149

Contents lists available at ScienceDirect

Optics Communications

journal homepage: www.elsevier.com/locate/optcom

2.7 W diffraction-limited yellow lasers by efficient frequency doubling of high-brightness tapered diode lasers

Mariafernanda Vilera [a,b,*], Mathias Christensen [a,b], Anders K. Hansen [b], Paranitharan Arulthasan [a], Danny Noordegraaf [a], Thomas Bußß [a], Ole B. Jensen [b], Peter E. Andersen [b], Peter M.W. Skovgaard [a]

[a] Norlase ApS, Brydehusvej 30, 2750 Ballerup, Denmark
[b] Technical University of Denmark, Department of Photonics Engineering, Frederiksborgvej 399, 4000 Roskilde, Denmark

ARTICLE INFO

Keywords:
Visible lasers
Tapered diode laser
Yellow lasers
Second harmonic generation
576 nm

ABSTRACT

Modulated yellow lasers may enable more efficient photocoagulation for treatments of ophthalmic diseases. In this regard, we present a laser system emitting 2.7 W of true-yellow light at 576 nm by frequency doubling the emission of a tapered diode laser emitting 7 W at 1153 nm. The frequency doubling is based on a single-pass configuration using a cascade of two 40-mm periodically poled lithium niobate (PPLN) crystals. The stabilization of the yellow power over 10 h showed a standard deviation of 0.10% and a relative intensity noise of 0.032% rms. Moreover, we demonstrate the generation of yellow pulses with 900 mW of amplitude and a high extinction ratio in the microsecond and millisecond regimes, as required for photocoagulation.

1. Introduction

High-brightness yellow lasers are seen as the next step in medical laser treatment of various diseases. Traditionally, most eye surgeries and eye treatments have been conducted by using green laser light to control blood coagulation [1,2]. However, the optimal wavelength for a particular photocoagulation application depends on the absorbers that are present in the area to be treated. For instance, using yellow light at 576 nm entails two advantages. First, it spectrally matches the main absorption peak of oxygenated hemoglobin. Second, for those patients suffering from cataracts, melanin absorption is lower than when using green light. These two characteristics make treatments involving longer wavelengths such as yellow light at 576 nm more efficacious [3]. The use of yellow lasers is not limited to medical treatments, it can also be beneficial in medical imaging, for instance, to excite fluorescent markers in Stimulated Emission Depletion Microscopy (STED) [4].

Yellow emission using semiconductor lasers can benefit from their well-known advantages, *i.e.*, high electro-optical conversion efficiency, compactness, and simplicity. Despite the recent advances reported for semiconductor lasers emitting at the yellow–orange range [5,6], the attained output power of few mW is still far from the required levels, usually in the Watt-range. This limitation has typically been circumvented by means of nonlinear processes such as second harmonic generation (SHG) or sum frequency generation (SFG) on several technologies, such as diode pumped solid state (DPSS) lasers, Raman lasers, fiber lasers and optically pumped semiconductor lasers (OPSL).

DPSS lasers have reached more than 1 W in the yellow–orange range [7–9] but at expenses of a low optical to optical conversion efficiency (≃ 10%). Raman lasers can also generate Watt-level yellow light together with a good beam quality [10,11], although they suffer from a low conversion efficiency, as in the case of DPSS lasers. Fiber lasers have shown outstanding performances with tens of Watts of yellow light and excellent beam quality [12–14]. However, these systems are rather complex and expensive, limiting their widespread use. OPSL lasers are promising sources thanks to the available wavelengths, tunability and modulation capability. They have demonstrated more than 8 W and 20 W at 578 nm [15] and 588 nm [16]. In spite of this, they require adequate and careful heat dissipation to manage such high-output power since only a fraction of the pump energy is converted to the desired wavelength [17].

Yellow emission can also be obtained by direct frequency doubling of diodes lasers. For efficient visible generation, the diode laser should emit a single longitudinal and lateral mode, exhibit spectral stability and good beam quality. Tapered diode lasers can successfully fulfill these requirements. Moreover the recent development of these devices at other infrared wavelengths such as 1154 nm [18] opened the possibility of addressing new visible wavelengths, in particular, at the yellow range. For instance, 860 mW of yellow light were generated by direct doubling the emission of a tapered diode laser in a waveguide nonlinear crystal [19]. Almost simultaneously with this work, 1.6 W at 576 nm were reported in [20] by doubling the emission of a hybrid

* Corresponding author at: Norlase ApS, Brydehusvej 30, 2750 Ballerup, Denmark.
E-mail address: mvilera@norlase.com (M. Vilera).

https://doi.org/10.1016/j.optcom.2018.11.052
Received 10 September 2018; Received in revised form 16 November 2018; Accepted 19 November 2018
Available online 22 November 2018

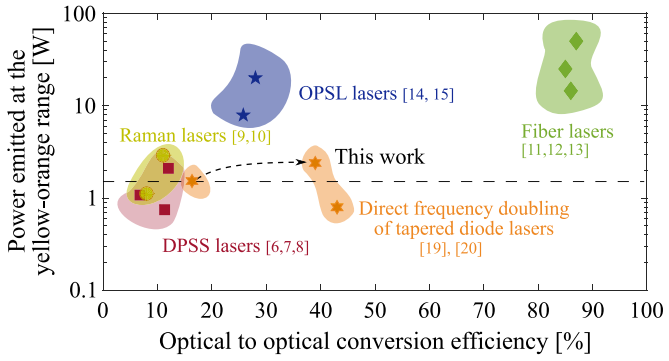

Fig. 1. Attained power by different technologies at the yellow–orange range as a function of the optical to optical conversion efficiency. The colored areas were plotted to guide the eye . (For interpretation of the references to color in this figure legend, the reader is referred to the web version of this article.)

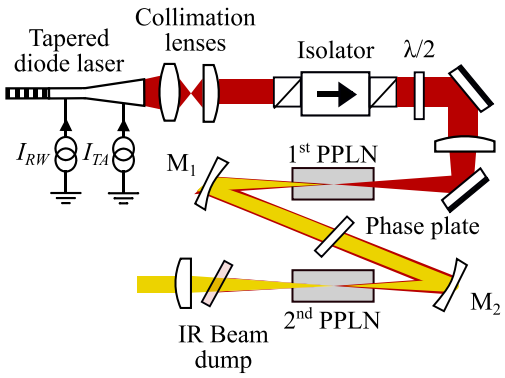

Fig. 2. Schematic representation of the experimental setup for generating yellow light . (For interpretation of the references to color in this figure legend, the reader is referred to the web version of this article.)

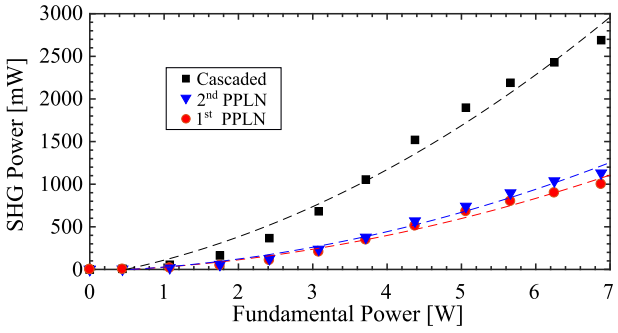

Fig. 3. SHG power as a function of the fundamental IR power. The temperature of the crystals was adjusted for each point of the curve.

all-semiconductor master-oscillator power-amplifier (MOPA). Although this result represents a noteworthy improvement in the attained yellow power, most of the commercial lasers used for photocoagulation deliver the expected power of 2 W [21] and therefore laser systems providing higher powers such as 2.7 W are needed to overcome potential system losses. From a technological point of view, the realization of miniaturized systems based on compact hybrid MOPAs is appealing, but the manufacturing and assembly process for placing the micro-optics and for coupling the light from the MO into the PA is challenging since nanometric tolerances are required.

For the previously mentioned technologies, Fig. 1 depicts the attained power at the yellow–orange range as a function of the optical to optical conversion efficiency. In dashed line, the latest power level achieved in [20] by a diode-based frequency doubling system. It is clear that within the diode-based technologies, our laser system shows an enhanced performance in terms of both power and conversion efficiency. Preliminary CW results of a 1-W yellow laser were reported by our group in [22]. In this work, we significantly increase the yellow output power up to 2.7 W while maintaining the near-diffraction-limited beam quality. This power increase drives our technology to power levels delivered by DPSS and Raman lasers but in addition, our laser system provides a higher conversion efficiency thus a clearly superior performance. Moreover, we report for the first time the generation of yellow pulses with 900 mW of peak power in the microsecond and millisecond regimes. This represents an increase of almost 4 times the yellow peak power achieved in [23] by modulating the SHG light of DBR tapered lasers and MOPAs.

2. Experimental setup

Fig. 2 shows the experimental setup used for the generation of yellow light at 576 nm by frequency doubling the emission of a tapered diode laser emitting at 1153 nm. A description of the experimental setup has been reported elsewhere [24] and therefore only the relevant features are repeated here. The tapered diode laser is a monolithically integrated device consisting of two sections: a ridge waveguide (RW) section with a distributed Bragg reflector (DBR), and a tapered amplifier (TA) section. The device emits a maximum of 7 W in a single longitudinal mode and a dominant spatial mode with a power content in the central lobe of approximately 67%. The chip was mounted p-side up with two separate contacts for driving the RW and TA sections. Details about the fabrication, geometry and epitaxial structure of these devices can be found in [19]. Due to the astigmatic character of the emitted beam by tapered diode lasers, two lenses were used for the collimation of the output beam: An aspheric lens for the fast (vertical) axis ($f = 2$ mm) and a cylindrical lens for the slow (horizontal) axis ($f = 5.8$ mm). Since the astigmatism depends on the TA current, the collimation of the slow axis was set for the maximum TA current, which in turns leads to the maximum SHG light. Both lenses were AR-coated for the infrared (IR) wavelength of interest. The collimated IR light was passed through an optical isolator to prevent unintended optical feedback to the diode laser. A half-wave plate was used to rotate the polarization to vertical in order to match the crystallographic Z-axis of both crystals. After that, the beam was steered using two plane mirrors, and focused into the first 40-mm periodically poled lithium niobate (PPLN) crystal using a lens ($f = 45$ mm). The two identical spherical mirrors (M_1, M_2, Radius $R = 100$ mm) refocus both the fundamental IR light and the SHG light. The phase plate in between compensates the phase mismatching between both IR and visible fields and maximizes the SHG light out of the second 40-mm PPLN crystal, as described in [25]. Finally, the remaining IR light was separated from the visible light using an IR beam dump.

3. Measurements

3.1. CW

Fig. 3 shows the SHG power as a function of the fundamental IR power for each crystal and for both in a cascaded configuration. The fundamental IR power was changed by sweeping the TA current. For each point of the curve, the temperature of the first and the second crystal, T_{C1} and T_{C2} respectively, were tuned to phase match both of them (cascaded) or only one of them at a time. The SHG power is expected to depend on the square power of the fundamental IR light (dashed lines). The small disagreement between the expected and the measured power values can be attributed to both the fixed position of the collimation of the slow axis and a deterioration of the beam quality at high output powers. The maximum IR power was 6.8 W when the tapered diode laser was driven at an RW current, $I_{RW} = 250$ mA, a TA

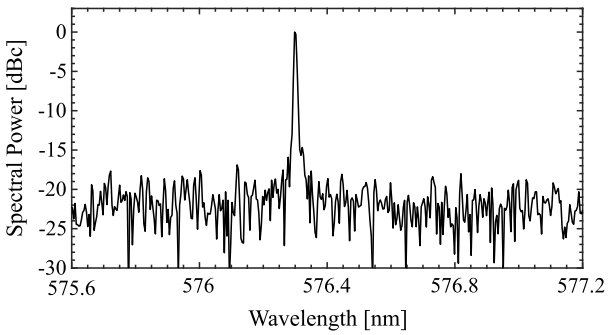

Fig. 4. Optical spectrum at the maximum SHG power. The driving currents for the tapered diode laser was I_{RW} = 250 mA and I_{TA} = 12 A. The temperature of the crystals were T_{C1} = 36 °C and T_{C2} = 35.7 °C.

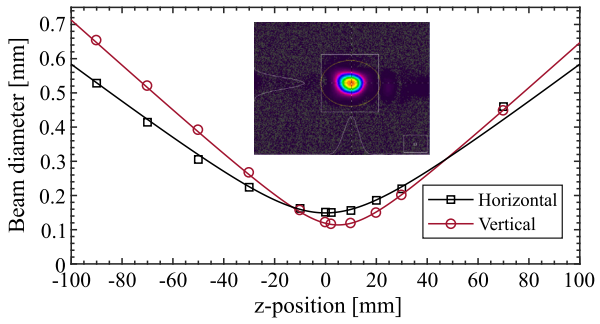

Fig. 5. Beam diameters according to the second order moments at 2.7 W yellow light. The inset shows an image of the beam at the focus.

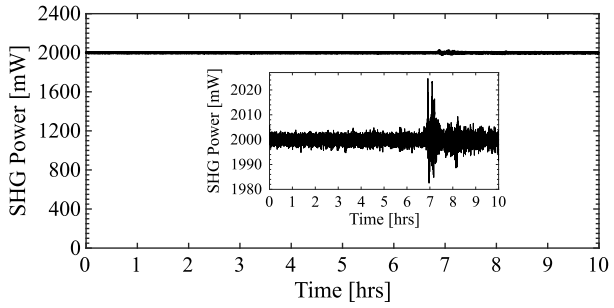

Fig. 6. Power stability over 10 h. The inset shows the same SHG power as a function of time but in a range of 45 mW. The power meter bandwidth was 100 kHz.

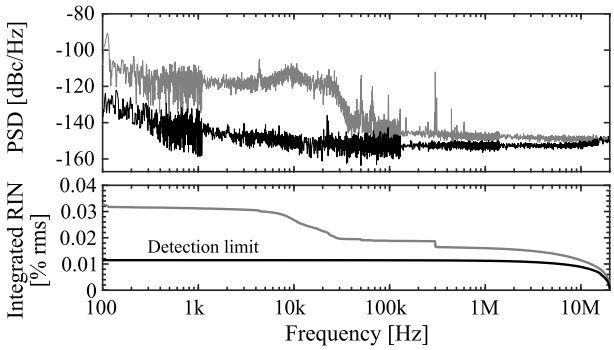

Fig. 7. Amplitude noise of the SHG light from both nonlinear crystals (top). Cumulative integrated RIN starting at 10 MHz and ending at 100 Hz (bottom). The SHG power was stabilized at 2 W (I_{RW} = 250 mA and I_{TA} = 12 A).

current, I_{TA} = 12 A and at a temperature of T = 18 °C. At this power level, the maximum SHG power was 1 W for the first crystal (T_{C1} = 36 °C), 1.1 W for the second crystal (T_{C2} = 35.1 °C), and 2.7 W for the cascaded crystals (T_{C1} = 36 °C, and T_{C2} = 35.7 °C). To the best of our knowledge, 2.7 W of yellow light represents the highest power generated in the yellow spectral region by direct frequency doubling the emission of a diode laser. In line with previous works, the cascaded SHG power is higher (~29%) than the sum of the attained powers by the individual crystals. The optical-to-optical efficiency was ~39%, whereas the wall-plug efficiency was 9.1% when considering the cooling and total consumption of the tapered diode laser and the heating of the crystals.

Fig. 4 shows the recorded optical spectrum for the SHG emission and for a yellow output power of 2.7 W. At this condition, the laser system exhibits single-mode emission at 576.3 nm with a high side-mode-suppression-ratio (SMSR) (> 19 dB). The spectral width of ~4 pm was limited by the resolution of the optical spectrum analyzer (OSA Advantest, Q8347).

The SHG light beam was characterized using a beam profiler (Ophir Photonics, Spiricon M2-200s). Fig. 5 depicts the beam caustics for the maximum SHG power of 2.7 W. The inset shows the focused beam profile. The beam quality factors $M^2_{4\sigma}$ based on the second moment criterion are 1.14 and 1.05 in the slow and fast axis, respectively.

The long-term stability of the SHG power was also investigated by means of an active feedback loop that tuned the temperature of the crystals while the tapered diode laser was kept at fixed injection conditions. This ensures that the modal quality of the tapered diode laser remains unchanged. Fig. 6 shows the SHG power over 10 h with a sampling period of 1 s The standard deviation was 2.064 mW, corresponding to 0.10% of the mean power (2 W).

The noise characteristics were measured according to the experimental method described in [26]. Fig. 7 depicts the amplitude power spectral density (PSD) at 2 W (gray line) together with the detection limit of the setup (black line). The integrated relative intensity noise (RIN) defined as the root mean square of the integrated PSD over a range of frequencies ([100 – 10M] Hz) is also shown. The integration range was set up to 10 MHz, value at which the amplitude signal equals the detection limit. The low RIN of the laser system is the result of the RIN of the low noise current supply (Norlase Aurora One) transferred to the tapered diode laser, and subsequently, to the second harmonic light. The total integrated RIN of 0.032% is in the same order of magnitude as the RIN values reported in low-noise commercial visible lasers (~0.02%) [26,27].

3.2. Modulation

The modulation of the second harmonic light is essential to address medical applications that are currently demanding microsecond and millisecond pulses [28,29]. In this regard, laser systems as described here can benefit from the inherent ability of diode lasers to be modulated over a wide range of frequencies. In practice, the direct modulation of the diode lasers gives rise to thermal fluctuations, which in turn modifies the refractive index and thus the emission wavelength. The difficulty is then to find an appropriate set of driving conditions at which the wavelength of the fundamental IR emission remains not only within the acceptance bandwidth of the crystals but also within the maximum SHG efficiency throughout the "on-state" of the pulse. Or alternatively, to use modulation schemes that benefit from the narrow and well-defined acceptance bandwidth, as described in [30] for MOPA devices. In order to illustrate this challenge, we first measure the acceptance bandwidth of both the individual crystals and the cascaded configuration, and we compare it with the expected longitudinal mode hop of the tapered diode laser. Fig. 8 shows the normalized SHG efficiency as a function of the wavelength drift of the tapered diode laser. The emission wavelength is 1153 nm. If a mode hop occurs by varying the currents of the tapered diode laser, the SHG efficiency will be reduced 15% for the single

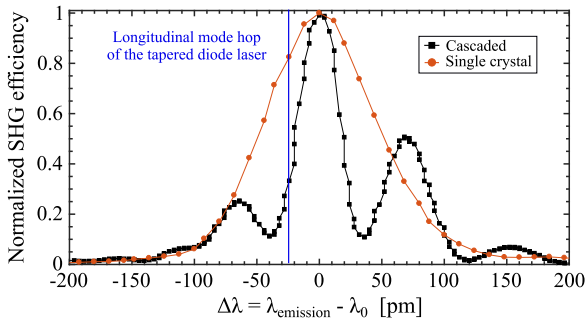

Fig. 8. Normalized SHG efficiency for the single crystals (orange circles) and for the cascaded configuration (black squares) relative to the wavelength drift $\Delta\lambda$. $\Delta\lambda$ is defined as the diode emission wavelength $\lambda_{emission}$ minus the central wavelength λ_0 = 1153 nm. Solid lines are drawn to guide the eye.

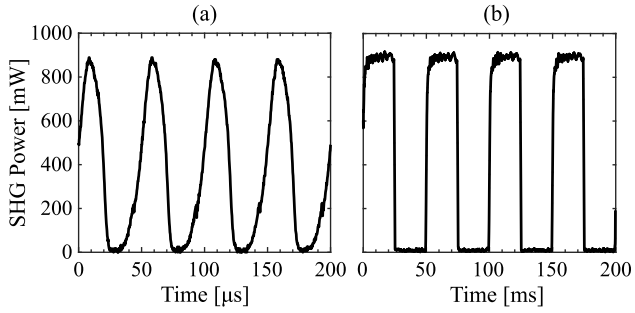

Fig. 9. Modulation results for two pulse durations T_{pulse} = 25 μs (a) and T_{pulse} = 25 ms (b). The CW conditions were I_{RW} = 300 mA, I_{TA} = [2, 10] A. The temperature of the PPLN crystal was T_{C1} = 34.8 °C.

crystal (orange line) and 65% for the cascaded crystals (black line). Usually, the sensitivity to mode-hopping of the tapered diode laser in the cascaded configuration precludes the generation of high-power visible pulses together with a high extinction ratio.

In our experiment, modulation was achieved by driving the RW section in the CW regime whereas an alternating current was injected into the TA section. The RW current was slightly increased to I_{RW} = 300 mA, value at which the pulses were stable. The alternating current was applied by using a voltage modulation input from the TA current supply (Arroyo Instruments, 4320). Modulation can also be attained by varying only the RW current, with the main disadvantage that the yellow light cannot be completely extinguished. Fig. 9 depicts the temporal response for the yellow light in the microsecond (a) and the millisecond (b) regimes when only the first crystal is at phase-matching. The rise and fall times are 15.4 and 8.8 μs, respectively. In the microsecond regime, the smoothing of the pulse shape is due to the frequency response of the driving electronics. In the millisecond regime, ripples at the top of the pulses can be observed. They are attributed to the shift of the fundamental wavelength around the maximum SHG efficiency of the crystal bandwidth. For both regimes, the optical modulation amplitude is almost 900 mW and the extinction ratio is 21 dB. Modulation using both cascaded crystals was possible provided that the maximum I_{TA} < 8 A. For higher values of I_{TA}, the yellow modulation proved to be challenging and is still under investigation.

4. Conclusions

In this work we present a laser system emitting 2.7 W of true-yellow light at 576 nm by cascaded frequency doubling of a tapered diode laser. The measurement of the beam profile of the second harmonic light shows beam quality factors of $M^2_{4\sigma}$ of 1.14 and 1.05 for the slow and fast axis, respectively. The stabilization of the second harmonic light during 10 h exhibits a standard deviation of 0.10% over 2 W. The integrated relative intensity noise from 100 Hz to 10 MHz is 0.0342%, comparable to the typical values for low-noise yellow lasers. We also demonstrate the generation of high-power yellow pulses of 900 mW of amplitude for the microsecond and millisecond regime with an extinction ratio larger than 20 dB. The performance of this yellow laser: Watt-power, good beam quality, low noise, modulation and power stability, has a great potential in future medical laser treatments.

Acknowledgments

This work has been funded by the Horizon 2020 Research and Innovation Framework Programme through the projects CoDiS (grant number, 734075) and MILAS (grant number, 739714), and the Innovation Fund Denmark (grant number, 5016-00076B).

References

[1] M.A. Latina, S.A. Sibayan, D.H. Shin, R.J. Noecker, G. Marcellino, Q-switched 532-nm Nd:YAG laser trabeculoplasty (selective laser trabeculoplasty): A multicenter, pilot, clinical study, Ophthalmology 105 (11) (1998) 2082–2090, http://dx.doi.org/10.1016/S0161-6420(98)91129-0.

[2] M. Nagpal, S. Marlecha, K. Nagpal, Comparison of laser photocoagulation for diabetic retinopathy using 532-nm standard laser versus multispot pattern scan laser, Retina 30 (3) (2010) 452–458, http://dx.doi.org/10.1097/IAE.0b013e3181c70127.

[3] S. Ryan, D. Hinton, S. Sadda, A. Schachat, Retina, 5th edition, Saunders, 2013.

[4] J.N. Farahani, M.J. Schibler, L.A. Bentolila, Stimulated Emission Depletion (STED) Microscopy: from Theory to Practice, Microsc. Sci. Technol. Appl. Educ. 2 (4) (2010) 1539–1547.

[5] J. Kasai, R. Akimoto, T. Hasama, H. Ishikawa, S. Fujisaki, S. Tanaka, S. Tsuji, Green-to-yellow continuous-wave operation of beznccdse quantum-well laser diodes at room temperature, Appl. Phys. Express 4 (8) (2011) 082102, http://dx.doi.org/10.1143/APEX.4.082102.

[6] N.N. Ledentsov, V.A. Shchukin, Y.M. Shernyakov, M.M. Kulagina, A.S. Payusov, N.Y. Gordeev, M.V. Maximov, A.E. Zhukov, T. Denneulin, N. Cherkashin, Room-temperature yellow-orange (In,Ga,Al)P-GaP laser diodes grown on (n11) GaAs substrates, Opt. Express 26 (11) (2018) 13985–13994, http://dx.doi.org/10.1364/OE.26.013985.

[7] J. Janousek, S. Johansson, P. Tidemand-Lichtenberg, S. Wang, J.L. Mortensen, P. Buchhave, F. Laurell, Efficient all solid-state continuous-wave yellow-orange light source, Opt. Express 13 (4) (2005) 1188–1192, http://dx.doi.org/10.1364/OPEX.13.001188.

[8] J.H. Liu, G.C. Sun, Y.D. Lee, All-solid-state continuous wave doubly linear resonator sum-frequency mixing yellow laser, Laser Phys. 22 (7) (2012) 1199–1201, http://dx.doi.org/10.1134/S1054660X12070079.

[9] Q. Fang, D. Lu, H. Yu, H. Zhang, J. Wang, Self-frequency-doubled vibronic yellow Yb:YCOB laser at the wavelength of 570 nm, Opt. Lett. 41 (5) (2016) 1002–1005, http://dx.doi.org/10.1364/OL.41.001002.

[10] A.J. Lee, H.M. Pask, J.A. Piper, H. Zhang, J. Wang, An intracavity, frequency-doubled $BaWO_4$ Raman laser generating multi-att continuous-wave, yellow emission, Opt. Express 18 (6) (2010) 5984–5992, http://dx.doi.org/10.1364/OE.18.005984.

[11] J. Jakutis-Neto, J. Lin, N.U. Wetter, H. Pask, Continuous-wave Watt-level Nd:YLF/KGW Raman laser operating at near-IR, yellow and lime-green wavelengths, Opt. Express 20 (9) (2012) 9841–9850, http://dx.doi.org/10.1364/OE.20.009841.

[12] Y. Feng, L.R. Taylor, D.B. Calia, 25 W Raman-fiber-amplifier-based 589 nm laser for laser guide star, Opt. Express 17 (21) (2009) 19021–19026, http://dx.doi.org/10.1364/OE.17.019021.

[13] L. Taylor, Y. Feng, D.B. Calia, High power narrowband 589 nm frequency doubled fibre laser source, Opt. Express 17 (17) (2009) 14687–14693, http://dx.doi.org/10.1364/OE.17.014687.

[14] L. Taylor, Y. Feng, D.B. Calia, 50W CW visible laser source at 589 nm obtained via frequency doubling of three coherently combined narrow-band Raman fibre amplifiers, Opt. Express 18 (8) (2010) 8540–8555, http://dx.doi.org/10.1364/OE.18.008540.

[15] S. Hilbich, W. Seelert, V. Ostroumov, C. Kannengiesser, R. v. Elm, J. Mueller, E. Weiss, H. Zhou, J. Chilla, New wavelengths in the yellow-orange range between 545 nm and 580 nm generated by an intracavity frequency-doubled optically pumped semiconductor laser, Proc.SPIE 6451 (2007) 6451 – 6451 – 7, http://dx.doi.org/10.1117/12.710571.

[16] E. Kantola, T. Leinonen, S. Ranta, M. Tavast, M. Guina, High-efficiency 20 W yellow VECSEL, Opt. Express 22 (6) (2014) 6372–6380, http://dx.doi.org/10.1364/OE.22.006372.

[17] M. Guina, A. Rantamäki, A. Härkönen, Optically pumped vecsels: review of technology and progress, J. Phys. D: Appl. Phys. 50 (38) (2017) 383001, http://dx.doi.org/10.1088/1361-6463/aa7bfd.

[18] D. Feise, F. Bugge, M. Matalla, A. Thies, P. Ressel, G. Blume, J. Hofmann, K. Paschke, Distributed Bragg reflector tapered diode lasers emitting more than 10 W at 1154 nm, Proc. SPIE 10514 (2018) 10514 – 10514 – 8, http://dx.doi.org/10.1117/12.2290658.

[19] R. Bege, G. Blume, D. Jedrzejczyk, K. Paschke, D. Feise, J. Hofmann, F. Bugge, G. Tränkle, Yellow laser emission at 578 nm by frequency doubling with diode lasers of high radiance at 1156 nm, Appl. Phys. B 123 (4) (2017) 1–11, http://dx.doi.org/10.1007/s00340-017-6700-4.

[20] A. Sahm, N. Werner, J. Hofmann, R. Bege, K. Paschke, Compact Miniaturized Laser Module Emitting More Than 1.6 W of Yellow Light at 576 nm, IEEE Photonics Technol. Lett. 30 (21) (2018) 1878–1881, http://dx.doi.org/10.1109/LPT.2018.2870524.

[21] IRIDEX IQ 577™/IQ 532™, Operator Manual, http://www.iridex.com/Portals/0/pdf/15510F_EN_IQ577-IQ532.pdf Accessed: 2018-11-16.

[22] M. Christensen, M. Vilera, D. Noordegraaf, A.K. Hansen, T. Buss, O.B. Jensen, P.M.W. Skovgaard, Diffraction-limited 577 nm true-yellow laser by frequency doubling of a tapered diode laser, Proc. SPIE 10516, Nonlinear Frequency Generation and Conversion: Materials and Devices XVII, 1051604, (February) (2018), 4, http://dx.doi.org.10.1117/12.2287377.

[23] N. Werner, J. Hofmann, A. Sahm, K. Paschke, Direct Modulation Capabilities of Micro-Integrated Laser Sources in the YellowGreen Spectral Range, IEEE Photonics Technol. Lett. 29 (12) (2017) 995–998, http://dx.doi.org/10.1109/LPT.2017.2700875.

[24] A.K. Hansen, M. Christensen, D. Noordegraaf, P. Heist, E. Papastathopoulos, V. Loyo-Maldonado, O.B. Jensen, P.M.W. Skovgaard, Efficient generation of 1.9 W yellow light by cascaded frequency doubling of a distributed Bragg reflector tapered diode, Appl. Opt. 55 (32) (2016) 9270–9274, http://dx.doi.org/10.1364/AO.55.009270.

[25] A.K. Hansen, M. Tawfieq, O.B. Jensen, P.E. Andersen, B. Sumpf, G. Erbert, P.M. Petersen, Concept for power scaling second harmonic generation using a cascade of nonlinear crystals, Opt. Express 23 (12) (2015) 15921–15934, http://dx.doi.org/10.1364/OE.23.015921.

[26] M. Tawfieq, A.K. Hansen, O.B. Jensen, D. Marti, B. Sumpf, P.E. Andersen, Intensity noise transfer through a diode-pumped titanium sapphire laser system, IEEE J. Quantum Electron. 54 (1) (2018) 1–9, http://dx.doi.org/10.1109/JQE.2017.2777860.

[27] R.P. Scott, C. Langrock, B.H. Kolner, High-dynamic-range laser amplitude and phase noise measurement techniques, IEEE J. Sel. Top. Quantum Electron. 7 (4) (2001) 641–655, http://dx.doi.org/10.1109/2944.974236.

[28] B. Gupta, M. Elagouz, D. McHugh, V. Chong, S. Sivaprasad, Micropulse diode laser photocoagulation for central serous chorio-retinopathy, Clin. Exp. Ophthalmol. 37 (8) (2009) 801–805, http://dx.doi.org/10.1111/j.1442-9071.2009.02157.x.

[29] N. Yadav, C. Jayadev, A. Mohan, P. Vijayan, R. Battu, S. Dabir, B. Shetty, R. Shetty, Subthreshold micropulse yellow laser (577 nm) in chronic central serous chorioretinopathy: safety profile and treatment outcome, Eye 29 (2) (2015) 258, http://dx.doi.org/10.1038/eye.2014.315.

[30] M. Christensen, A.K. Hansen, D. Noordegraaf, O.B. Jensen, P.M.W. Skovgaard, Deep modulation of second-harmonic light by wavelength detuning of a laser diode, Appl. Opt. 56 (8) (2017) 2250–2254, http://dx.doi.org/10.1364/AO.56.002250.